Sustainable Food Technology

ROYAL SOCIETY OF CHEMISTRY

PAPER

View Article Online
View Journal | View Issue

Cite this: *Sustainable Food Technol.*, 2025, 3, 1450

Effects of vibro-milling time and sintering temperature on the formation and selected properties of nano-hydroxyapatite ceramics derived from bovine bone

Anirut Raksujarit[a] and Tanagorn Sangtawesin *[b]

Received 25th October 2024
Accepted 9th July 2025

DOI: 10.1039/d4fb00322e

rsc.li/susfoodtech

Hydroxyapatite (HA) bioceramics require nanoscale powders to achieve the mechanical strength necessary for load-bearing implants. The impact of vibro-milling on HA derived from bovine bone remains unclear. This study hypothesized that varying vibro-milling duration and sintering temperature could optimize the nano-HA characteristics and ceramic performance. Natural bovine bone was processed into HA powder through boiling, calcination at 800 °C, and initial ball milling. The resulting HA powder was then vibro-milled for 0, 1, 2, 4, and 8 hours to generate nanopowders and sintered between 1150 °C and 1300 °C. A 2 hours vibro-milling treatment produced uniform nano-HA (<100 nm) with good crystallinity. Sintering temperature had a greater influence than milling time, with 1250 °C treatment yielding the highest densification and a maximum bending strength of ~112 MPa. These findings demonstrate that a 2 hours vibro-milling step combined with 1250 °C sintering produces HA ceramics suitable for load-bearing applications.

Sustainability spotlight

Our research directly supports the United Nations Sustainable Development Goals, particularly SDG 12 (Responsible Consumption and Production), by demonstrating how bovine bone, a by-product of the food industry, can be repurposed into valuable nano-hydroxyapatite ceramics. This process not only reduces waste but also enhances resource efficiency within the food and materials sectors. Furthermore, by contributing to SDG 9 (industry, innovation, and infrastructure), our innovative vibro-milling and sintering techniques advance sustainable industrial processes. Additionally, this work supports SDG 3 (good health and well-being) by improving the quality and effectiveness of biomedical materials, potentially reducing the environmental impact of healthcare practices and promoting well-being through sustainable materials science. Thus, our research exemplifies a multidisciplinary approach to achieving sustainability targets through the innovative utilization of food industry by-products.

1 Introduction

Globally, over 130 million metric tons of waste animal bones are generated annually from the food industry and household sources.[1] Hydroxyapatite (HA, $Ca_{10}(PO_4)_6(OH)_2$) and bone char from bone waste are valuable catalysts in processes such as biodiesel production and hydrocracking. Furthermore, HA used in medicine, orthopaedics, and dentistry shows biocompatibility and bioactivity, surpassing alternative bone substitute materials made from metal alloys or other ceramic materials.[2–4]

Unlike caprine and galline bones—which begin to decompose into β-tricalcium phosphate (β-TCP) at temperatures above 750 °C and 700 °C, respectively, leading to phase impurities—bovine bone maintains a single-phase hydroxyapatite (HA) even up to 1000 °C, owing to its superior thermal stability and crystallinity.[5] Additionally, bovine-derived HA maintains a Ca/P ratio near 1.67 and achieves ~25% porosity with ~387 MPa hardness at 750 °C—properties that are similar to those of human cortical bone—while caprine HA risks excessive densification and galline HA remains overly porous.[5] These attributes make bovine bone the superior precursor for HA production, offering many advantages such as lower cost and greater availability for mass production.[6–9] Other elements, including carbonate, magnesium, and sodium, were detected only in trace amounts,[9] which could benefit a material used in the human body.

However, fresh bovine bone contains inorganic parts of HA, some organic parts primarily composed of collagen, and a small number of proteins. Impurities and fat are typically removed from bone by prolonged boiling, autoclaving and subcritical water processing.[7,9] Calcination is then used to decompose the remaining collagen or other organic compounds at a temperature between 750 °C and 1000 °C.[6] Vibro-milling is a mechanical

[a]*Department of Physics and General Science, Faculty of Science and Technology, Chiang Mai Rajabhat University, Chiang Mai 50300, Thailand*

[b]*Thailand Institute of Nuclear Technology (Public Organization), Headquarters 9/9 Moo 7, Sai Mun, Ongkharak, Nakhon Nayok 26120, Thailand. E-mail: tanagorn@tint.or.th*

deproteinization method in which bone undergoes high-frequency oscillations in a liquid medium, breaking down the organic matrix and reducing particle size without extreme heat. This process preserves HA's nanostructure, shortens processing time, and lowers energy consumption, although a brief, low-temperature calcination step is typically required afterward to achieve full crystallinity.[9–12] By combining efficient impurity removal with minimal thermal impact, vibro-milling delivers fine, near-pure HA while maintaining its desirable nanoscale features.

Numerous studies have highlighted that achieving optimal mechanical performance in HA bioceramics requires nano-hydroxyapatite (nHA) powders.[13–16] Owing to their high specific surface area, nHA powders enhance sinterability and densification, leading to improved fracture toughness and other key mechanical properties essential for load-bearing applications.[13,17,18] However, successful sintering depends not only on reducing particle size but also on controlling particle size distribution and morphology.[19] Moreover, the inadvertent formation of secondary phases such as alpha tricalcium phosphate (α-TCP) and beta-tricalcium phosphate (β-TCP) during processing can substantially compromise the mechanical integrity of HA ceramics. Consequently, developing methods to produce nHA powders while preventing the emergence of these unwanted phases has become a critical challenge in HA ceramic fabrication.[20]

The study presents a sustainable approach to synthesizing nano-hydroxyapatite (nHA) ceramics by using bovine bone, an abundant by-product from the meat industry. This valorization of agricultural waste aligns with the principles of the circular economy by reducing environmental burdens associated with bone disposal. The work demonstrates that appropriate control of vibro-milling time and sintering temperature allows for the production of HA ceramics with desirable mechanical properties, suitable for biomedical applications such as bone grafts and catalysts. The use of naturally derived precursors offers a low-cost and potentially lower-emission alternative to conventional synthetic routes, suggesting an eco-friendlier method of ceramic fabrication.

2 Experimental procedures

2.1 Sample preparation

The HA powder was produced from natural bovine bone (a butcher house in Chang Klan Subdistrict, Mueang Chiang Mai District, Thailand) by a sequence of thermal processes. Fresh bovine bones were cut into smaller pieces and rinsing with tap water and a wire brush to remove macroscopic adhering impurities. Then, the samples were boiled in distilled water for eight hours to remove bone marrow and tendons. After that, the deproteinization was continued by boiling in distilled water. The samples were then dried overnight at 200 °C. After that, the samples were heated at 800 °C for 3 h in an alumina crucible at a heating and cooling rate of 4 °C min^{-1} to destroy the disease-causing agents. The obtained samples were crushed and milled with ethanol in a polyethylene container using yttria-stabilized zirconia balls as the grinding media for 24 h, followed by sieving through a 325-mesh screen to obtain the HA powder.

Then, 50 g of HA powder was reground by a vibro-milling method (McCrone Micronizing Mill, Germany) in ethanol with yttria-stabilized zirconia balls. The vibro-milling time was varied from 0 to 8 h. After vibro-milling, the slurry was dried for 24 h. The obtained powders were then uniaxially pressed into a disc shape of 15 mm diameter and 2.5 mm thickness under a pressure of 50 MPa. The resulting green pellets were sintered in an alumina crucible under atmospheric pressure at 1150–1300 °C for 2 h at a heating and cooling rate of 4 °C min^{-1} to room temperature.

2.2 Sample characterization

X-ray diffraction technique (XRD Philip X'pert, Netherlands) with Cu K (λ = 0.154 nm) was used to identify the phase formation, and 2θ was in the range from 10° to 60°. The densities were tested by Archimedes' method, using distilled water as the fluid medium. The microstructure evaluation was investigated by scanning electron microscopy (SEM: JEOL JSM6335F, France). The ceramics were polished with silicon carbide abrasive paper from coarse to fine before the mechanical measurements. The hardness was measured using a Vickers microhardness tester (Struers Duramin 0.01). Indentations were applied on the polished surfaces with a major load of 0.98 N and an indentation period of 15 s. The bending strength of the ceramics was determined using a ball-on-ring tester.[21] The strength was calculated using the following expression:

$$\sigma = \frac{3F(1+\nu)}{4\pi t^2}\left[\frac{(1-\nu)}{(1+\nu)} \times \frac{2a^2-b^2}{2R^2} + 2\ln\left(\frac{a}{b}\right) + 1\right] \quad (1)$$

where σ is the strength expressed in MPa, ν is the Poison ratio, F is the breaking load in Newton, R is the radius of the measurement samples, a is the radius of the support, t is the thickness of the measurement sample, and b is $t/3$.

3 Results and discussion

3.1 Effects of vibro-milling times on the HA ceramic properties

The densities of sintered HA as a function of vibro-milling time at sintering temperatures of 1200 °C and 1300 °C are shown in

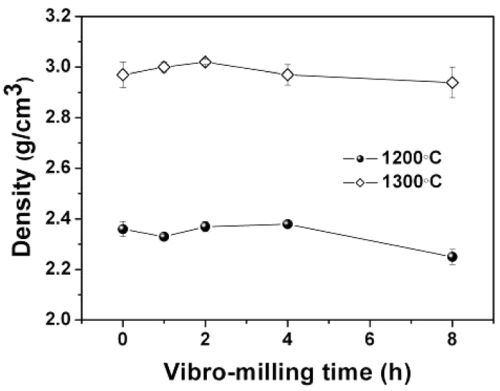

Fig. 1 Density as a function of vibro-milling time for HA ceramics sintered at 1200 °C and 1300 °C.

Fig. 1. The density of the sintered HA at 1200 °C (2.25–2.39 g cm^{-3}) was significantly lower than that at 1300 °C (2.94–3.01 g cm^{-3}), which is close to the values from other reports.[13] It can be explained that the HA powder was incompletely sintered at 1200 °C, but the elimination of porosity during the final sintering stage was found at 1300 °C, resulting in approximately 20% denser than that at 1200 °C.

Notably, the HA densities slightly increased at a milling time of 2 h, an effect of nano needle-like structures, as reported in our previous work.[10] The nanocrystals can increase the HA sinterability at elevated temperatures. However, at over 8 h of milling time, the HA densities slightly dropped. This result suggested that the sintering temperature has a more significant effect on densification than the vibro-milling time.

Fig. 2 shows the fracture surfaces of the HA samples after sintering at 1200 °C at different vibro-milling times. The HA ceramics presented a porous structure depending on the vibro-milling time. The densest structure was observed for the 2 hours-milling time sample, as shown in Fig. 2c, which agrees with the density results. Furthermore, needle-like nanostructures were observed in the HA samples milled for 2–4 hours. This structure was proposed to improve the mechanical properties of HA.[9] Furthermore, Fig. 3 shows the SEM image of the HA grains (vibro-milled at 2 and 4 h). It shows that nanocrystalline crystals penetrated from the grain to the grain boundary regions. However, at the vibro-milling time of 8 hours, the nanocrystalline HA exhibited excessive growth with micrometer needle-like HA grains (Fig. 2e), resulting in a drop in the HA densities.

Fig. 4 shows the fracture surfaces of the HA samples after sintering at 1300 °C with different vibro-milling times. The result shows that a full-liquid phase occurred in the HA samples, presented as a glass-like structure of the fracture surface. The presence of a glass-like structure gave rise to higher density values at 1300 °C than at 1200 °C, and most of the pores

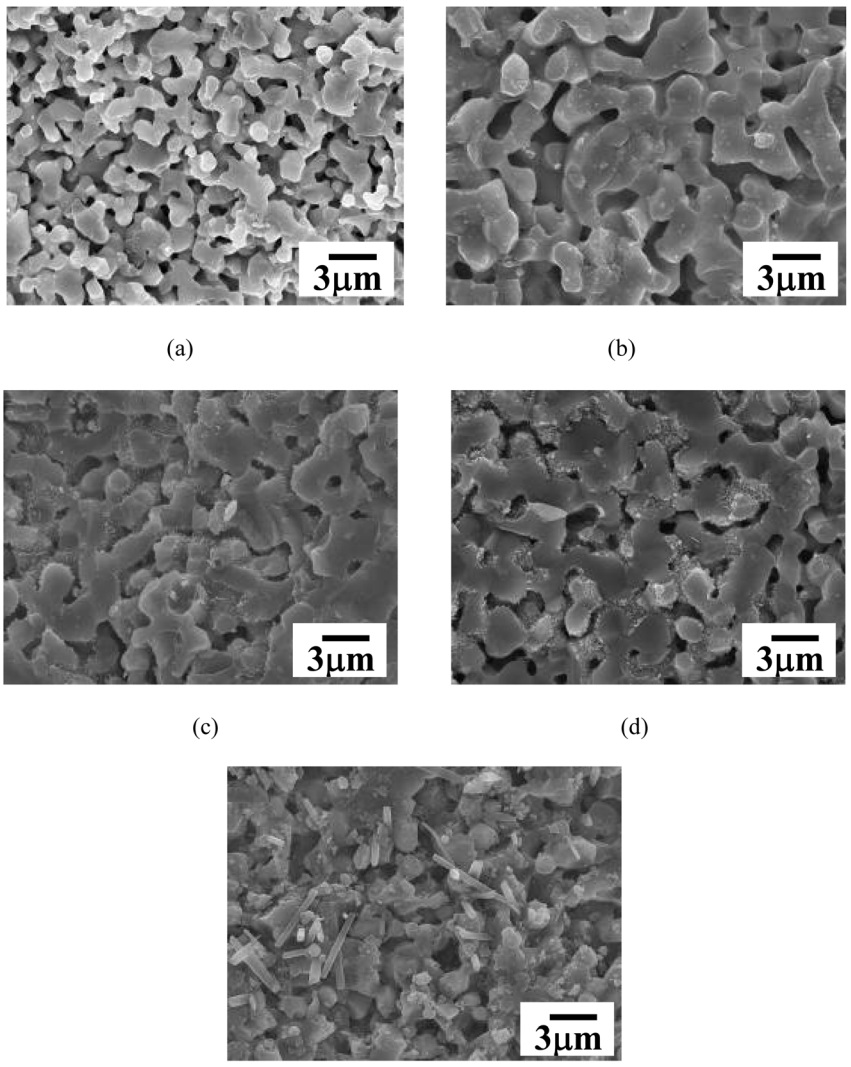

Fig. 2 Fracture surfaces of various HA ceramics sintered at 1200 °C for various vibro-milling times: (a) 0 h, (b) 1 h, (c) 2 h, (d) 4 h, and (e) 8 h.

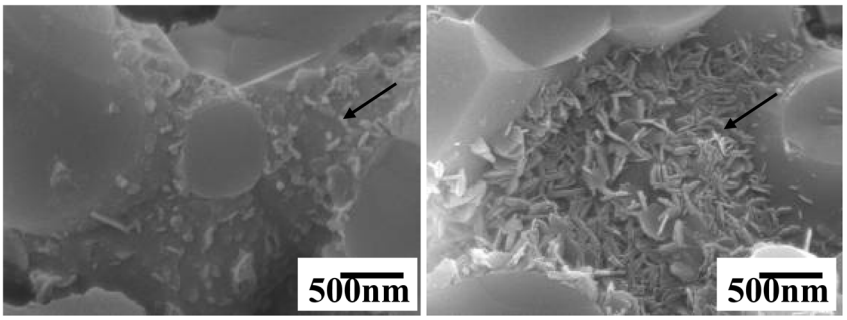

Fig. 3 Fracture surfaces of HA ceramics sintered at 1200 °C for vibro-milling times of: (a) 2 h and (b) 4 h. Arrows indicate that the nanostructure HA grains embedded in the micron-sized grains.

were eliminated. Therefore, the 1300 °C or higher sintering temperature is unsuitable for retaining the nanocrystalline structure within the HA grains.

Fig. 5 shows the Vickers hardness data as a function of the vibro-milling time of the HA ceramics. Vickers hardness data indicated that vibro-milling time has a significant effect on the

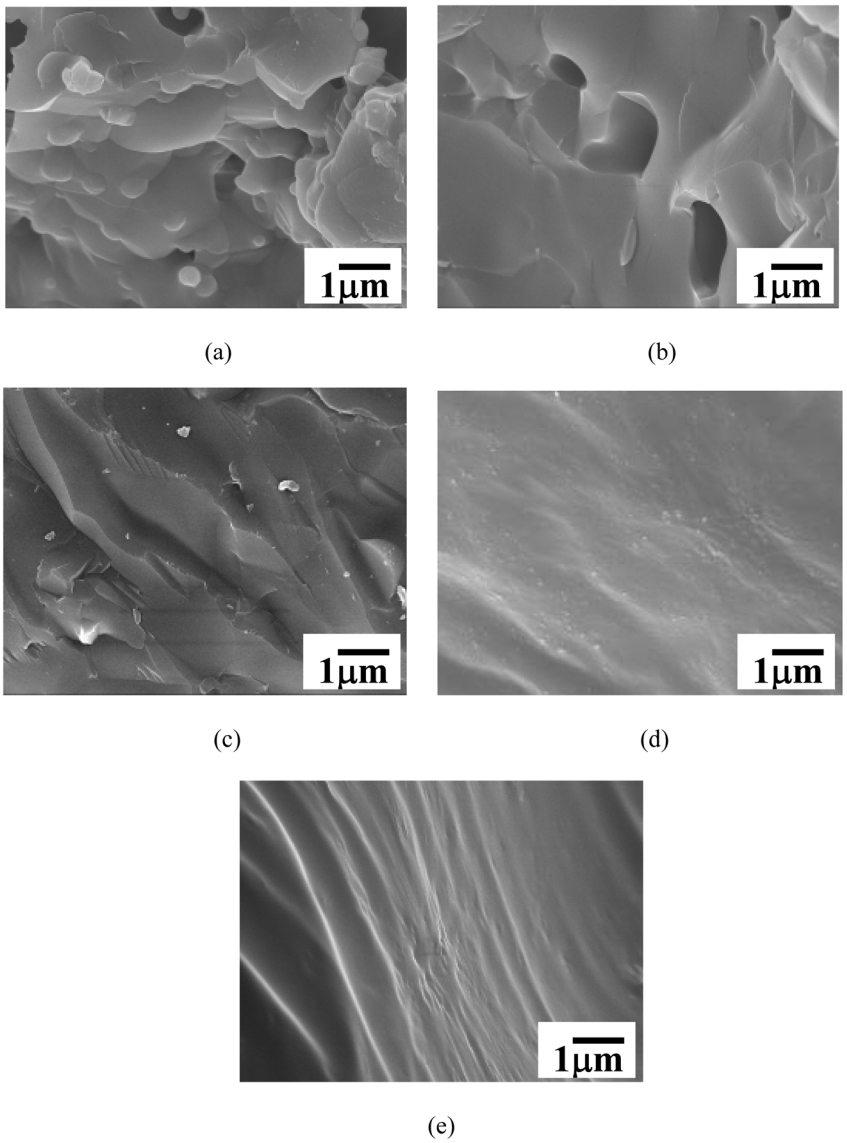

Fig. 4 Fracture surfaces of HA ceramics sintered at 1300 °C for various vibro-milling times: (a) 0 h, (b) 1 h, (c) 2 h, (d) 4 h, and (e) 8 h.

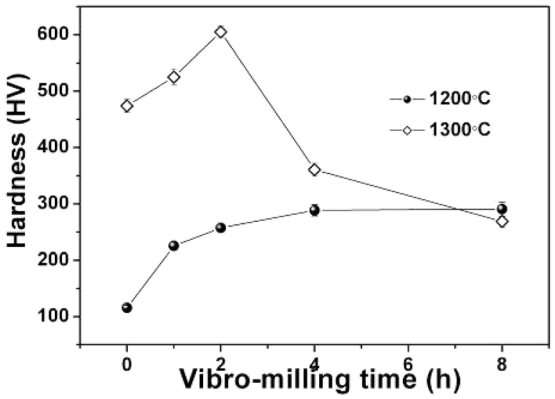

Fig. 5 Effect of vibro-milling time on the Vickers hardness of HA ceramics sintered at 1200 °C and 1300 °C.

mechanical properties of the HA ceramic samples. At 1200 °C, there was a sharp increase from ~120 HV (0 h of vibro-milling) to 230 HV (2 h of vibro-milling) and gradually increased to 290 HV (4 h of vibro-milling). Notably, the hardness of the HV samples did not follow the same trend as their densities. Although the 8 h of vibro-milling exhibited the lowest density, it had the highest hardness, while this sample possessed the maximum hardness value. It is believed that the high hardness value for this sample may be due to the formation of a rod-like structure embedded in the grain as confirmed by the SEM image (Fig. 3), which can act as a reinforced structure in ceramics. For the higher sintering temperature of 1300 °C, initially, the trend was similar to that of the 1200 °C sample until 2 h of milling; after that, the values decreased abruptly for the samples milled for 4 and 8 hours. This fall-off is consistent with the density result.[22] However, the highest hardness value of about 605 could be observed for the sample vibro-milled at 2 h.

Fig. 6 shows the flexural bending strength *versus* the milling time. For the samples sintered at 1300 °C, the maximum flexural bending strength (54.9 MPa) was observed for the sample milled for one hour. The higher flexural bending strength was found at 1200 °C with 2 h milling (69.0 MPa), which is about two times higher than that of the 0 hours-milled sample (34.9 MPa). Moreover, this value closely approximates the values found for the cortical bone of the rabbit femur (88 MPa), an often-used animal model.[23] It can be assumed that the lower strength of the 1200 °C samples milled at 4 and 8 h was due to the increase in pores and loosely compact HA grains as observed by SEM (Fig. 2d and e).

Moreover, the previous report revealed that the critical sintering temperature for HA is 1300 °C,[24] and the HA structure tends to collapse at a temperature greater than 1300 °C. In this work, the resulting strength of the sintered HA nanoceramics at 1300 °C was poor compared to their HA micro-ceramic counterparts (0 hours vibro-milling). Nanoscale HA ceramics tend to reduce the sintering temperature compared to the conventional HA ceramics. Consequently, it can be assumed that the ceramics made from the nanoscale HA powder possess a higher strength and a lower optimum sintering temperature, overcoming that of the micron-scale HA ceramics, promising a bright future to use as bone substitute materials.

3.2 Effect of the sintering temperature on the properties of HA ceramics

The 2 hours-milled powder gave rise to the HA ceramic's optimum densification and mechanical properties. Further, the sintering temperature was found to have a substantial effect on the ceramic's properties of the HA ceramics. The effect of sintering temperature on the properties of HA ceramics was investigated, and the additional properties of these HA ceramics are reported in this section.

Fig. 7 shows the XRD patterns of the sintered HA powders. The main phase of HA was found, and impurity peaks were located at 32° and 47°, identified as beta-tricalcium phosphate (β-TCP), which was reported as the ionic substitution enhancing the ceramic's bioactivity.[25] The β-TCP phases were found at sintering temperatures of 1150 °C, 1200 °C, 1250 °C, and 1350 °C (Fig. 7). Notably, the intensity of β-TCP peaks increased according to sintering temperatures. At 1300 °C, a third phase was found at 31°, indexed as an alpha-tricalcium phosphate (α-

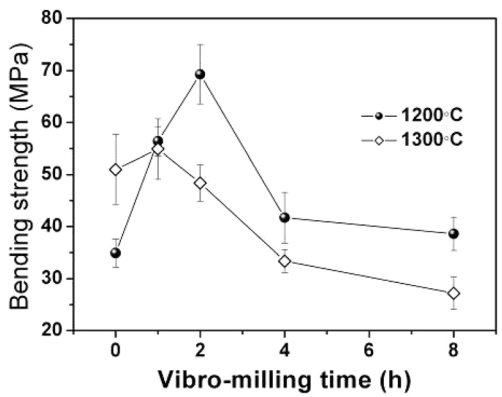

Fig. 6 Effect of vibro-milling time on the flexural bending strength of HA samples sintered at 1200 °C and 1300 °C.

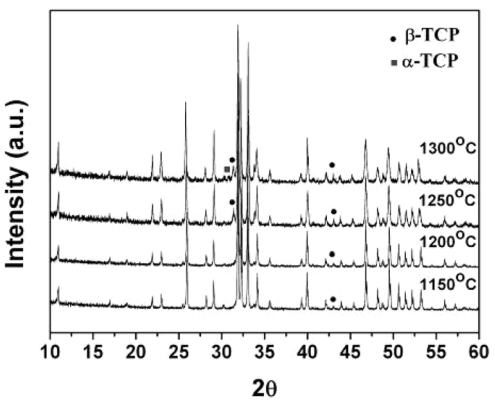

Fig. 7 X-ray diffraction patterns of 2 hours-milled HA ceramics after sintering at 1150, 1200, 1250 and 1300 °C.

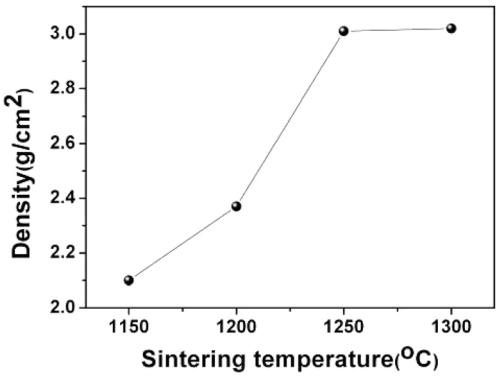

Fig. 8 Density as a function of sintering temperature for the HA ceramics made from 2 hours-vibro-milled nano-powder.

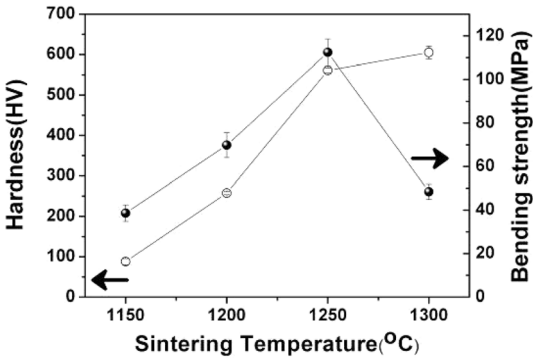

Fig. 10 Hardness (HV) and bending strength of HA samples sintered at various sintering temperatures.

TCP). The formation of β-TCP and (α-TCP) was due to a gradual loss of the radical OH^- (dehydroxylation) in the HA structure during heating in air at a temperature above 800 °C.[26]

Fig. 8 shows the density of the HA ceramics, vibro-milled for 2 h, as a function of the heating temperature. The ceramic exhibited a low density at 1150 °C and a sharp increase at 1250 °C. The density slightly increased at 1300 °C with a maximum density of 3.020 g cm^{-3}, which is ~44% higher than that at 1150 °C.

Fig. 9 shows the SEM images of fracture surfaces of HA ceramics at various sintering temperatures. The ceramics presented a high porosity for the sintering below 1250 °C; micropores were observed, and nanocrystals also occurred at grain boundaries. It proved that the milled HA powder consists of nano-particles. At a temperature higher than 1250 °C, a dense microstructure was observed. The grains formed a rod-shaped structure at 1200 °C and grew larger (1.0 × 1.5 mm) at 1250 °C with submicron pores. Nanorod crystals can be formed by increasing the calcination temperature and grow to micrometres in size.[27] Generally, the HA crystal has a hexagonal structure ($P6_3/m$ symmetry) with the lattice parameters of $a = b = 9.42$ Å and $c = 6.88$ Å (c/a is about 0.73), and prefers to grow in the c-axis direction due to the needle-like or rod shape of the obtained particle after processing.[28]

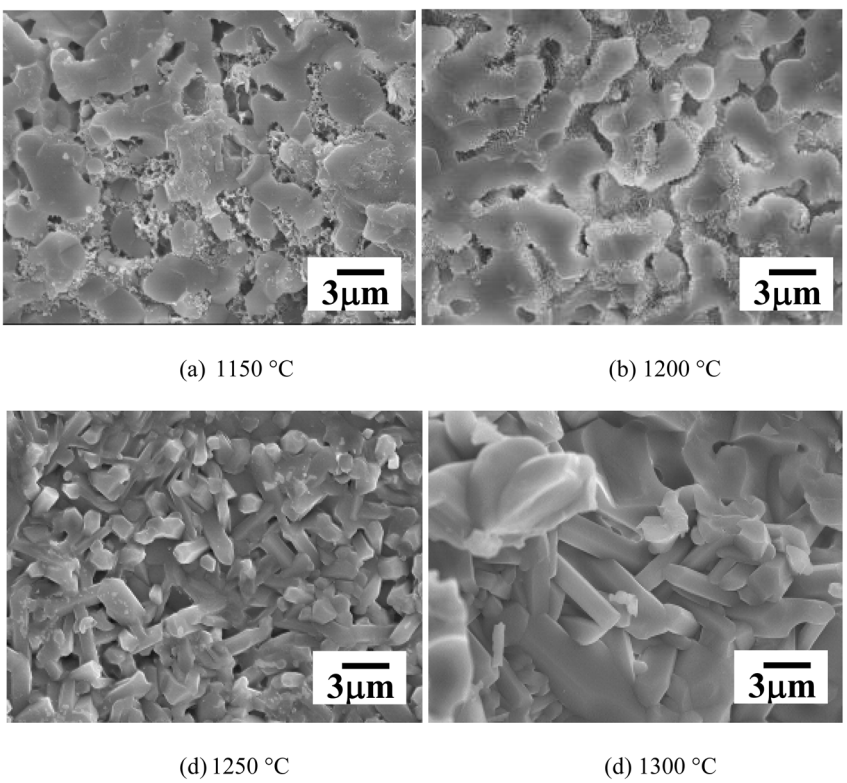

Fig. 9 SEM micrographs of the fracture surface of HA samples sintered at (a) 1150 °C, (b) 1200 °C, (c) 1250 °C and (d) 1300 °C.

Table 1 Summary of hydroxyapatite and nanocrystalline hydroxyapatite syntheses

Sources	Product	Preparation methods	Ref.
Bovine bone	Porous hydroxyapatite	Calcined bone powder at 900 °C for 3 h	29
Bovine bone	Hydroxyapatite supported $ZnCl_2$	Calcined bone powder at 800 °C for 6 h Mixed with zinc choline solution by stirring	30
Bovine bone	Nanocrystalline hydroxyapatite	Calcined bone powder at 800 °C for 3 h Vibro milling at 0–8 h	10
Bovine bone	Nanocrystalline hydroxyapatite	Calcined bone powder at 800 °C for 3 h Vibro milling for 0–8 h Annealed at 1150–1300 °C for 2 h	This work
Calcium hydroxide, di-ammonium hydrogen orthophosphate and calcium sulfate	Nanocrystalline hydroxyapatite	Pulsed laser YAG laser 532 nm, 1064 nm, 0–35 kHz	31
Calcium carbonate and orthophosphate supplies	Nanocrystalline hydroxyapatite	Chemical method, stirring with CO_2 flow	32

Further, our previous work[10] reported that the HA powder derived from natural bovine bones exhibited nanorod particles. This result also supports the preferred orientation in information in the *c*-axis direction. Therefore, the rod-shaped grains observed in the present work are attributed to the grain growth process; for example, the nanorod particles grew and developed into micrometre-sized rod grains.

The effect of sintering temperature on the hardness and bending strength was studied, and the results are shown in Fig. 10. It can be seen that the bending strength and hardness strongly depended on the sintering temperature. The remarkable difference in the sintering ability of the nano-sized HA powders resulted in significant differences in the microstructure, bending strength and hardness values. The sintering temperature increased, and the bending strength and hardness values changed linearly and then reached the maximum (112.4 $\pm$ 6.2 MPa) at 1250 °C. However, it dropped abruptly to 48.4 $\pm$ 3.5 MPa at 1300 °C. However, the hardness increased slightly to 605 $\pm$ 16.0 HV at 1300 °C. An increase in the hardness may be due to the reduction of porosity as the sintering temperature increases, which can also be confirmed by the microstructures in the SEM results (Fig. 9). However, the slight change in hardness value from 1250 to 1300 °C indicates that the liquid phase sintering occurred at high temperatures. It can be noted that the presence or absence of porosity in ceramics significantly affects the mechanical properties. However, for the bending strength, it was conversely observed that the bending strength value dramatically reduced at 1300 °C even though this ceramic sample has low porosity. The rule of a glassy phase on the mechanical properties may be explained. The presence of the glass favored densification, and hence, hardness property was enhanced. Nevertheless, excess glass content can cause probably over-firing effects at elevated sintering temperatures.[22] This glass residual, which is usually a very fragile material and sensitive to any defects, may cause a reduction in the bending strength value at 1300 °C.

This present study clearly demonstrated that the size of HA powders and sintering temperatures significantly affected the densification, microstructure, and mechanical properties of the resulting ceramics. While nano needle-shaped particles embedded in nano-sized grains enhanced the mechanical performance—achieving a maximum flexural strength of 112 MPa at 2 hours vibro-milling and 1250 °C—challenges remain. Sintering above 1200 °C led to excessive grain coarsening, loss of nano-features, and formation of β-TCP and α-TCP phases, which may compromise long-term stability. Additionally, the absence of biocompatibility testing and concerns regarding milling consistency and scalability limit the immediate application in biomedical fields. Nevertheless, this simple and low-cost vibro-milling technique holds strong potential for developing HA ceramics for artificial bone applications with further optimization.

Table 1 highlights various synthesis methods for hydroxyapatite (HA), particularly focusing on the use of bovine bone as a sustainable and natural calcium source. Compared to other studies that employed simple calcination[29] or chemical mixing with metal salts such as $ZnCl_2$,[30] this work adopts a combined approach involving calcination at 800 °C, followed by vibro-milling (0–8 hours) and sintering at 1150–1300 °C. This method not only produces nanocrystalline HA with controlled crystallite size and enhanced mechanical properties but also aligns with sustainability goals by valorizing the animal bone waste—an abundant by-product of the food industry. Unlike synthetic chemical precursor-based methods involving lasers[31] or chemical reactions with CO_2 flow,[32] the current approach is more environmentally friendly, cost-effective, and suitable for scale-up. Thus, this work stands out for integrating waste valorization, energy-efficient processing, and high-performance material production, supporting both biomedical functionality and circular economy principles.

4 Conclusions

The vibro-milling method provides a simple route for preparing nanoneedle-like hydroxyapatite powders from natural bovine bone with low cost, reproducibility, and high mass productivity. The effect of vibro-milling time on the physical and mechanical properties of the HAP ceramic has been revealed. It was found

that the vibro-milling time slightly affects the ceramic's density and mechanical density. However, the 2 hours of vibro-milling time was the optimum condition for further investigation with finer steps of sintering temperatures from 1150, 1200, 1250, and 1300 °C. The results indicated that the sintering temperature strongly affected the sintered HA ceramics' density, hardness, and bending strength. The optimum processing parameters were found as 2 h of vibro-milling at 1250 °C sintering temperature, as the resulting ceramics possess the highest value of density of 3.01 g cm^{-3}, a maximum bending strength of 112 MPa, and a considerable hardness value of 605 HV, which meet the desired values of artificial bone applications.

Data availability

All data supporting the findings of this article are presented in the manuscript's tables and figures. No restrictions apply to the availability of these data.

Author contributions

Anirut Raksujarit: conceptualization, methodology, visualization, resources, writing-original draft, review & editing, project administration, and funding acquisition. Tanagorn Sangtawesin: conceptualization, methodology, resources, writing-original draft, review & editing, and funding acquisition.

Conflicts of interest

The authors declare that they have no known competing financial interests or personal relationships that could have influence the work reported in this paper.

Acknowledgements

The authors would like to thank the Thailand Research Fund, the Thailand Office of the Higher Education Commission, the National Metal and Materials Technology Center (MTEC), and the Faculty of Science, Chiang Mai University, for financial support.

References

1 A. Hart, K. Ebiundu, E. Peretomode, H. Onyeaka, O. F. Nwabor and K. Obileke, Value-added materials recovered from waste bone biomass: technologies and applications, *RSC Adv.*, 2022, **12**(34), 22302–22330.
2 R. Murugan and S. Ramakrishna, Development of nanocomposites for bone grafting, *Compos. Sci. Technol.*, 2005, **65**(15), 2385–2406.
3 K. Hing, Bone repair in the twenty-first century: Biology, chemistry or engineering?, *Philos. Trans. R. Soc., A*, 2004, **362**, 2821–2850.
4 W. Suchanek, M. Yashima, M. Kakihana and M. Yoshimura, Hydroxyapatite/Hydroxyapatite-Whisker Composites without Sintering Additives: Mechanical Properties and Microstructural Evolution, *J. Am. Ceram. Soc.*, 1997, **80**(11), 2805–2813.
5 S. Ramesh, Z. Z. Loo, C. Y. Tan, W. J. K. Chew, Y. C. Ching, F. Tarlochan, H. Chandran, S. Krishnasamy, L. T. Bang and A. A. D. Sarhan, Characterization of biogenic hydroxyapatite derived from animal bones for biomedical applications, *Ceram. Int.*, 2018, **44**(9), 10525–10530.
6 C. Y. Ooi, M. Hamdi and S. Ramesh, Properties of hydroxyapatite produced by annealing of bovine bone, *Ceram. Int.*, 2007, **33**(7), 1171–1177.
7 N. A. M. Barakat, M. S. Khil, A. M. Omran, F. A. Sheikh and H. Y. Kim, Extraction of pure natural hydroxyapatite from the bovine bones bio waste by three different methods, *J. Mater. Process. Technol.*, 2009, **209**(7), 3408–3415.
8 F. H. Lin, C. J. Liao, K. S. Chen and J. S. Sun, Preparation of a biphasic porous bioceramic by heating bovine cancellous bone with Na4P2O7.10H2O addition, *Biomaterials*, 1999, **20**(5), 475–484.
9 A. G. Adhikara, A. P. Maharani, A. Puspitasari, N. F. Nuswantoro, D. Juliadmi, M. A. J. Maras, D. B. Nugroho, B. Saksono and G. Gunawarman, Bovine hydroxyapatite for bone tissue engineering: Preparation, characterization, challenges, and future perspectives, *Eur. Polym. J.*, 2024, **214**, 113171.
10 A. Ruksudjarit, K. Pengpat, G. Rujijanagul and T. Tunkasiri, Synthesis and characterization of nanocrystalline hydroxyapatite from natural bovine bone, *Curr. Appl. Phys*, 2008, **8**(3), 270–272.
11 E. Rashidi, H. Rezaie and H. Ghassai, The effect of carbon nanotube addition on the mechanical properties and biological functionality of poly-ether-ether-ketone–hydroxyapatite composites, *Polym. Compos.*, 2021, **42**(7), 3253–3261.
12 W. Chaisan, R. Yimnirun and S. Ananta, Effect of vibro-milling time on phase formation and particle size of barium titanate nanopowders, *Ceram. Int.*, 2009, **35**(1), 173–176.
13 S. Kalita, A. Bhardwaj and H. Bhatt, Nanocrystalline Calcium Phosphate Ceramics in Biomedical Engineering, *Mater. Sci. Eng., C*, 2007, **27**, 441–449.
14 S. Bose and S. K. Saha, Synthesis of Hydroxyapatite Nanopowders *via* Sucrose-Templated Sol–Gel Method, *J. Am. Ceram. Soc.*, 2003, **86**(6), 1055–1057.
15 P. K. Chu, J. Y. Chen, L. P. Wang and N. Huang, Plasma-surface modification of biomaterials, *Mater. Sci. Eng., R*, 2002, **36**(5), 143–206.
16 F. Chen, Z.-C. Wang and C.-J. Lin, Preparation and characterization of nano-sized hydroxyapatite particles and hydroxyapatite/chitosan nano-composite for use in biomedical materials, *Mater. Lett.*, 2002, **57**(4), 858–861.
17 M. R. Ayatollahi, M. Y. Yahya, H. Asgharzadeh Shirazi and S. A. Hassan, Mechanical and tribological properties of hydroxyapatite nanoparticles extracted from natural bovine bone and the bone cement developed by nano-sized bovine hydroxyapatite filler, *Ceram. Int.*, 2015, **41**(9, Part A), 10818–10827.

18 M. Du, J. Chen, K. Liu, H. Xing and C. Song, Recent advances in biomedical engineering of nano-hydroxyapatite including dentistry, cancer treatment and bone repair, *Composites, Part B*, 2021, **215**, 108790.
19 A. Banerjee, A. Bandyopadhyay and S. Bose, Hydroxyapatite nanopowders: Synthesis, densification and cell–materials interaction, *Mater. Sci. Eng., C*, 2007, **27**(4), 729–735.
20 S. Zhang and K. E. Gonsalves, Preparation and characterization of thermally stable nanohydroxyapatite, *J. Mater. Sci.: Mater. Med.*, 1997, **8**(1), 25–28.
21 A. F. Kirstein and R. M. Woolley, Symmetrical bending of thin circular elastic plates on equally spaced point supports, *Journal of Research of the National Bureau of Standards, Section C: Engineering and Instrumentation*, 1967, 1.
22 G. Goller and F. Oktar, Sintering Effects on Mechanical Properties of Biologically Derived Dentine Hydroxyapatite, *Mater. Lett.*, 2002, **56**, 142–147.
23 E. Landi, A. Tampieri, G. Celotti, R. Langenati, M. Sandri and S. Sprio, Nucleation of biomimetic apatite in synthetic body fluids: dense and porous scaffold development, *Biomaterials*, 2005, **26**(16), 2835–2845.
24 G. Goller, H. Demirkiran, F. Oktar and E. Demirkesen, Processing and characterization of bioglass reinforced hydroxyapatite composites, *Ceram. Int.*, 2003, 721–724.
25 S. J. Kalita, S. Bose, H. L. Hosick and A. Bandyopadhyay, CaO–P2O5–Na2O-based sintering additives for hydroxyapatite (HAp) ceramics, *Biomaterials*, 2004, **25**(12), 2331–2339.
26 A. Raksujarit, K. Pengpat, G. Rujijanagul and T. Tunkasiri, Processing and properties of nanoporous hydroxyapatite ceramics, *Mater. Des.*, 2010, **31**(4), 1658–1660.
27 Y. Han, S. Li, X. Wang, L. Jia and J. He, Preparation of hydroxyapatite rod-like crystals by protein precursor method, *Mater. Res. Bull.*, 2007, **42**(6), 1169–1177.
28 M. Vallet-Regí and J. M. González-Calbet, Calcium phosphates as substitution of bone tissues, *Prog. Solid State Chem.*, 2004, **1–2**, 1–31.
29 J. Wadthanakul, S. Phanrawee, B. Narongdech, C. Komsanti, R. Chamnan, B. Waraporn, C. Nopakarn, T. Kriangkrai and G. Rujijanagul, Investigation of the bioactivity and antibacterial activity of porous hydroxyapatite ceramics derived from natural sources, *J. Asian Ceram. Soc*, 2025, **13**(1), 116–125.
30 R. Azzallou, O. Ouerghi, M. H. Geesi, Y. Riadi, M. A. Taleb, R. Mamouni, S. Lazar, A. Kaiba, M. Kamal and S. Villain, Bovine bone-derived natural hydroxyapatite-supported ZnCl2 as a sustainable high efficiency heterogeneous biocatalyst for synthesizing amidoalkyl naphthols, *J. Phys. Chem. Solids*, 2022, **163**, 110533.
31 S. Shaikh, S. Gupta, A. Mishra, P. A. Sheikh, P. Singh and A. Kumar, Laser-assisted synthesis of nano-hydroxyapatite and functionalization with bone active molecules for bone regeneration, *Colloids Surf., B*, 2024, **237**, 113859.
32 V. Naubnome, A. Prihanto, W. W. Schmahl, Y. M. Pusparizkita, R. Ismail, J. Jamari and A. P. Bayuseno, Chemical precipitation of nanocrystalline hydroxyapatite with calcium carbonate derived from green mussel shell wastes and several phosphorus sources, *Case Stud. Chem. Environ. Eng.*, 2025, **11**, 101154.